J. Fluid Mech. (1996), *vol.* 311, *pp.* 153–176

Natural ventilation of an enclosure containing two buoyancy sources

By P. COOPER[1] AND P. F. LINDEN[2]

[1] Department of Mechanical Engineering, University of Wollongong, Wollongong, NSW 2522, Australia

[2] Department of Applied Mathematics and Theoretical Physics, Silver Street, Cambridge CB3 9EW, UK

(Received 1 February 1994 and in revised form 20 October 1995)

This paper describes experiments and theoretical modelling of a naturally ventilated enclosure containing two point sources of buoyancy. Previous work on the flow and stratification that develop in a space owing to the presence of a single source of buoyancy has been extended to cover two sources of positive or negative buoyancy in an attempt to produce more realistic models of practical problems. Examples include naturally ventilated buildings, and industrial or medical processes involving dispersal of contaminants by air currents. The experimental technique involves the use of a water-filled enclosure with salt solution injected at two points. These sources of negative buoyancy form turbulent plumes within the enclosure. Two sources of unequal strength are found to produce a vertical density profile consisting of three distinct, fully mixed layers. The paper describes a theoretical model that successfully predicts the depths and densities of these layers. The positions of the interfaces between the three layers were found to be a function only of the effective area A^* of the enclosure openings, the height of the enclosure H and the *ratio* of the strengths of the two sources of buoyancy B_1/B_2. The behaviour of a system with one source of positive buoyancy at the lower boundary and one of negative buoyancy at the upper boundary of the enclosure is also examined. This case has particular relevance to the prediction of thermal stratification in rooms with both cold and warm surfaces present. Again the height of the interfaces is dependent only on the geometry of the enclosure and the source strength ratio. Three distinct types of flow pattern are predicted and observed.

1. Introduction

Natural ventilation of enclosures is an important topic in several areas of engineering, particularly in the building industry. It is often desirable to use naturally ventilated systems as far as possible, both to reduce energy consumption and to minimize the level of airborne pollutants within a building. Additionally, contaminants such as fumes or dust generated from processes within industrial premises must be controlled. The sizing and location of ventilation openings in a naturally ventilated building are crucial in ensuring an adequate indoor climate and providing sufficient fresh air to the occupants.

The research findings reported here form a part of a wider effort to develop relatively simple models of the fluid flow within enclosures with internal sources of heat or buoyancy. Most buildings have complex geometries and the turbulent flows generated within the buildings are very difficult to compute. Laboratory experiments and relatively simple theoretical models have proved to be successful in providing insights

into these flows, and have given information that can be used by designers to help develop efficient ventilation systems.

The use of internal sources of buoyancy to generate a ventilation flow within a building is becoming a popular means of providing a comfortable working environment. The harnessing of the natural buoyancy that is generated is energy efficient, and in many modern buildings, which are of tight construction and with high areas of glazing, the input of buoyancy within the space is often sufficient to drive a naturally ventilated flow provided the appropriate design features are properly incorporated. Many modern building types are designed with these features in mind. One example is the atrium which allows solar radiation to enhance the internal sources of buoyancy produced by, for example, occupants and equipment, to generate significant thermal stratification within the space. The warmest air accumulates near the ceiling of the atrium and strong stable stratification develops. If such a space has openings at high and low levels this buoyant fluid will drive an upward displacement ventilation, with warm air leaving through the upper level openings and cool ambient air flowing in at lower levels. This flow produces a region at the base of the space which is at ambient temperature. The simplest design criterion is to ensure that the depth of this base layer is higher than the occupied zone so that all occupants are surrounded by air at ambient temperature. The heat within the building is then flushed upwards out of the occupied zone by this displacement ventilation and extracted through the roof of the building. This mode of ventilation is a very efficient one for removing heat and waste products.

In an attempt to understand this flow and to provide simple rules for design criteria we have investigated simple models of this ventilation regime. Linden, Lane-Serff & Smeed (1990) investigated the flow in an enclosure with high-level and low-level openings generated by a single point source of buoyancy on the floor of the enclosure. They showed that in this case a very simple stratification develops consisting of two layers separated by a horizontal interface. The lower layer is at uniform ambient temperature and the upper layer is also at a uniform temperature which depends on the buoyancy flux from the source. In an enclosure of height H the dimensionless depth of the cool ambient layer $\xi = h/H$ is given by

$$\frac{A^*}{H^2} = C^{3/2}\left(\frac{\xi^5}{1-\xi}\right)^{1/2}, \tag{1}$$

where A^* is the 'effective' area of the top and bottom openings of the enclosure, and H is the height difference between the top and bottom openings.† The constant $C = \frac{6}{5}\alpha(\frac{9}{10}\alpha)^{1/3}\pi^{2/3}$, where α is the entrainment constant for the plume.

The effective area A^* of the openings is defined as

$$A^* = \frac{c_d a_t a_b}{\left(\frac{1}{2}\left(\frac{c_d^2}{c}a_t^2 + a_b^2\right)\right)^{1/2}}, \tag{2}$$

where a_t and a_b are the areas of the top and bottom openings, respectively, and c is the pressure loss coefficient associated with the inflow through a sharp-edged opening. A discharge coefficient c_d is used here to account for the vena contracta arising at the downstream side of the sharp-edged upper vents. If there are n sources of equal

† It has recently been brought to our attention by G. G. Rooney that this expression was first derived independently by Thomas *et al.* (1963).

strength present on the floor of the enclosure, again a two-layer stratification forms and the non-dimensional height of the interface, ξ, is given by

$$\frac{1}{n}\frac{A^*}{H^2} = C^{3/2}\left(\frac{\xi^5}{1-\xi}\right)^{1/2}. \tag{3}$$

In the single plume case or when the sources have equal strength, the height of the interface is independent of the buoyancy fluxes and depends only on the dimensionless vent area A^*/H^2. On the other hand the temperature of the upper layer, which is independent of height, increases as the heat flux of the plumes increases.

These results provide some simple guidelines for the designer. Equations (1) and (3) show that in order to achieve a deep layer at ambient temperature ($\xi \to 1$) it is necessary to have a very large number of openable vents. In practice this is extremely difficult to achieve, and consequently it is a good idea to have some dead space at the top of an enclosure in which the hot air can accumulate in order to drive the flow. The flow through the system is controlled by the effective area given in (2), and the magnitude of A^* is determined by the smaller vent area. For example when $a_t \ll a_b$, $A^* \to a_t c_d \sqrt{2}$, and so control of the flow can be achieved by adjusting the smaller openings to the enclosure. A further feature of these flows is that the interface height is independent of the strength of the buoyancy flux from the source, which results from the fact that the position of the interface is governed by the entrainment into the plume.

Thermal stratification (or stratification of contaminant concentration) in practical situations does not generally exhibit a sharp change in density between two internally well-mixed layers as described in the simple model above. A more gradual change is observed from ambient conditions at the bottom of the enclosure to a maximum temperature at the top (e.g. see Gorton & Sassi 1982; Jacobsen 1988; Cooper & Mak 1991). This type of stratification arises owing to many factors which are not included in the simplified model of a single plume within the space. In practice, heating occurs owing to distributed sources of buoyancy of different strengths, located at various positions within the space.

In an attempt to address this issue the approach of Linden *et al.* (1990) has been extended to cover multiple sources of buoyancy of different strengths. The fluid mechanics are similar to the single source case but the analysis is complicated by the fact that the stronger plumes rise through a stratified region and discharge their buoyancy at higher levels within the space. In order to analyse this situation we examine the flow in two stages. The first stage of the analysis, described in this paper, is to determine the flow driven by two unequal sources of buoyancy. In this case the stronger plume rises through a layer of different density from the environment which is produced by the weaker plume, and it is necessary to calculate the flow of the stronger plume in this layer by treating it in a manner similar to that of Morton (1959) in his paper on 'forced plumes', i.e. plumes evolving from sources of both finite volume and momentum flux – such flows are also referred to as buoyancy jets (see List 1979). An exact solution for the two-plume problem is found here and compared with some experiments. On the basis of this comparison we then extend the analysis to multiple sources in a companion paper (Linden & Cooper 1996). From the analysis shown in the present paper, we see that it is possible but very difficult to generalize the two-plume results exactly to the case of multiple plumes, and consequently, we seek an approximate method of solution which simplifies the analysis considerably. This is described in detail in Linden & Cooper (1996).

The format of the present paper is as follows. In §2 the case of two plumes with buoyancy of the same sign is analysed. It is shown that a three-layer stratification

develops in the steady-state, and the heights of the two interfaces are determined. The case where the buoyancy fluxes in the two plumes have opposite signs is considered in §3. The results of experiments which test the theory are presented in §4, a discussion of these results and the conclusions are given in §5.

2. Two-plumes with buoyancy of the same sign

2.1. *Conservation relations*

A schematic diagram of two point sources of positive buoyancy forming plumes in a ventilated enclosure is shown in figure 1. It is postulated that three layers of fluid of different densities are formed (and this configuration is confirmed by the experiments described in §4). Both sources (B_1 and B_2, with $B_1 < B_2$ for definiteness) are assumed to be 'ideal point sources' in that they each release a finite quantity of buoyancy (equivalent to heat in the thermal situation) but zero mass and momentum; i.e. they produce 'unforced plumes'. These plumes develop through layer 0 which has the same density as the ambient fluid. A distinct interface then occurs at $z = h_1$ where the weaker plume mixes with layer 1 and the reduced gravity g'_1 in the layer is assumed to be equal to that of the plume G'_1 at that level. (Upper case letters denote plume quantities, lower case letters denote environment quantities.) The stronger plume from source B_2 passes through layer 1 and mixes with layer 2 at height $z = h_2$, where $G'_2 = g'_2$. It is assumed that the horizontal separation of the two plumes is sufficient to ensure they develop independently. Furthermore, it is assumed that all the fluid of the stronger plume passes through the upper interface as observed visually in experiments described in §4. Although plumes have a Gaussian buoyancy distribution in the temporal mean, the intermittent nature of the flow at the plume boundary means buoyant elements within the plume arrive less often but cross the interface almost as easily as in the centre of the plume.

The volume flux through the top and bottom openings is then given by

$$Q_t = Q_b = A^*(g'_2(H-h_2)+g'_1(h_2-h_1))^{1/2}. \tag{4}$$

This equation relates the volume of flow driven through the openings by the hydrostatic head resulting from the stratification within the space, and follows directly from Bernoulli's theorem and is a simple extension of the result given in Linden *et al.* (1990), equation (2.4), for a two-layer stratification.

Following the approach of Morton, Taylor & Turner (1956) and Morton (1959), we use the entrainment assumption to model flow in the plumes. This assumption states that the ratio of the mean speed of inflow of external fluid at the edge of a plume to the mean vertical velocity of the plume is a constant, α. This assumption is equivalent to similarity when the ambient fluid is unstratified. Furthermore, 'top hat' distributions of vertical velocity, W, and buoyancy, G', are used; the values of these quantities are assumed constant across the plume and are, therefore, functions only of height, z.

Given this form of the flow a number of volume flux, buoyancy flux and density relations may then be identified. Since the only vertical transfer of fluid across the stable interfaces takes place within the plumes, steady state conservation of volume flux implies

$$Q_t = Q_b = Q_{22} = Q_{11}+Q_{21}. \tag{5}$$

[*Note*: the first term of the double subscripts refers to the plume and the second term to the interface, e.g. Q_{21} is the volume flux in plume 2 passing through interface 1 between layers 1 and 2, see figure 1].

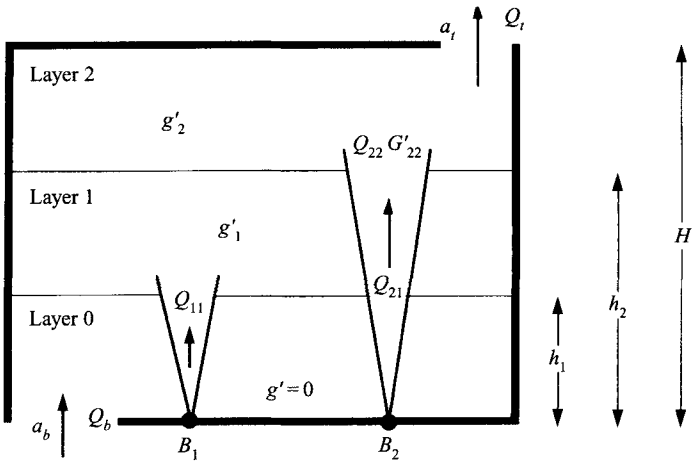

FIGURE 1. Ventilated enclosure with two positive buoyancy sources.

In a steady state the buoyancy fluxes into and out of each of the layers are equal and hence

$$B_1 + B_2 = Q_{11}\,G'_{11} + Q_{21}\,G'_{21} = Q_{22}\,G'_{22}. \tag{6}$$

In the lower layer (layer 0), in which the density is constant (at the ambient value), the buoyancy fluxes within each plume are constant (Morton *et al.* 1956). For the weaker plume

$$B_1 = G'_1\,Q_1 = \text{constant}, \tag{7}$$

and volume flux and reduced gravity at $z = h_1$ are given by

$$Q_{11} = C(B_1\,h_1^5)^{1/3}, \tag{8}$$

$$G'_{11} = \frac{1}{C}(B_1^2\,h_1^{-5})^{1/3} = g'_1, \tag{9}$$

respectively. As stated above $C = \frac{6}{5}\alpha(\frac{9}{10}\alpha)^{1/3}\,\pi^{2/3}$, where α is the entrainment constant for the plume.

Equivalent relations hold for the strong plume in layer 0,

$$B_2 = G'_2\,Q_2 = \text{constant}, \tag{10}$$

$$Q_{21} = C(B_2\,h_1^5)^{1/3}, \tag{11}$$

$$G'_{21} = \frac{1}{C}(B_2^2\,h_1^{-5})^{1/3}. \tag{12}$$

The behaviour of the stronger plume in layer 1 is influenced by the fact that it experiences a step change in the surrounding fluid density at $z = h_1$. We have modelled this by considering the plume to consist of two parts. The first part consists of an 'unforced' plume in layer 0. The second part is a 'distributed' plume of finite volume flux and finite momentum flux originating at $z = h_1$ and developing in an environment of uniform reduced density, g'_1. This upper part of the plume has a reduced buoyancy flux, B'_2, relative to its surroundings which is given by

$$B'_2 = B_2 - g'_1\,Q_{21}, \tag{13}$$

which is constant with height in layer 1. This plume continues to rise until it reaches layer 2 at $z = h_2$ at which point

$$G'_{22} = g'_2. \tag{14}$$

Equations (5), (8) and (11) may be rearranged to obtain

$$Q_{22} = Q_{11}(1+(B_2/B_1)^{1/3}). \tag{15}$$

Substituting (6), (14) and (15) into (4) we have

$$Q_{11}\left(1+\left(\frac{B_2}{B_1}\right)^{1/3}\right) = A^*\left(\frac{(B_1+B_2)}{Q_{11}(1+(B_2/B_1)^{1/3})}(H-h_2)+G'_{11}(h_2-h_1)\right)^{1/2}.$$

Then using (6) and (8) gives

$$\frac{A^*}{H^2C^{3/2}} = \frac{(1+\psi^{1/3})^{3/2}}{(1+\psi)^{1/2}}\left(\frac{(h_1/H)^5}{1-h_1/H-\dfrac{(1-\psi^{2/3})}{(1+\psi)}\left(\dfrac{h_2-h_1}{H}\right)}\right)^{1/2}, \tag{16}$$

where $\psi \equiv B_1/B_2 \leqslant 1$ is the ratio of the buoyancy fluxes. For a fixed geometry we postulate that on dimensional grounds it is possible to define the ratio of the two interface heights as

$$h_2/h_1 = 1+f(\psi), \tag{17}$$

where $f(\psi)$ is some function of the ratio of source strengths, $\psi = B_1/B_2$, to be determined. This relationship reflects the departure from the single plume case, so that $f(0) = 0$. Then (16) becomes

$$\frac{A^*}{H^2C^{3/2}} = \frac{(1+\psi^{1/3})^{3/2}}{(1+\psi)^{1/2}}\left(\frac{\xi_1^5}{1-\xi_1-\dfrac{(1-\psi^{2/3})}{(1+\psi)}f(\psi)\,\xi_1}\right)^{1/2}, \tag{18}$$

where $\xi_n = h_n/H, n = 1, 2$.

This result agrees with that of Linden *et al.* (1990) in the following limiting cases. For a single plume (i.e. $\psi = 0$), (17) implies that $f(\psi) = 0$ and the result for the single interface height that forms is as given in (1). For two plumes of equal strength (i.e. $\psi = 1$) the density step between layers 1 and 2 vanishes and the single interface height, h_1, is as given in (3) with $n = 2$.

2.2. *Analysis of the 'distributed' plume*

In order to determine $f(\psi)$ and the interface positions it is necessary to consider the behaviour of the strong plume when it passes through the lower interface, $z = h_1$, and its subsequent motion through layer 1. In this layer the plume buoyancy flux is constant but is reduced from its original value as a result of the density step at the interface (see (13)). The behaviour of plume 2 in layer 1 can be considered to be that of a plume from an area source of finite volume and momentum flux originating at $z = h_1$, developing in an environment of uniform density. The model used for this analysis is shown in figure 2.

As before, a plume originating from a source may be treated as having uniform velocity and density across any horizontal cross-section (i.e. 'top hat' profiles). The differential equations governing flow in such a buoyant plume are (see, for example, Caulfield 1991)

$$\frac{\mathrm{d}\hat{Q}}{\mathrm{d}z} = 2\alpha M^{1/2}, \quad \frac{\mathrm{d}M^2}{\mathrm{d}z} = 2F\hat{Q}, \tag{19a, b}$$

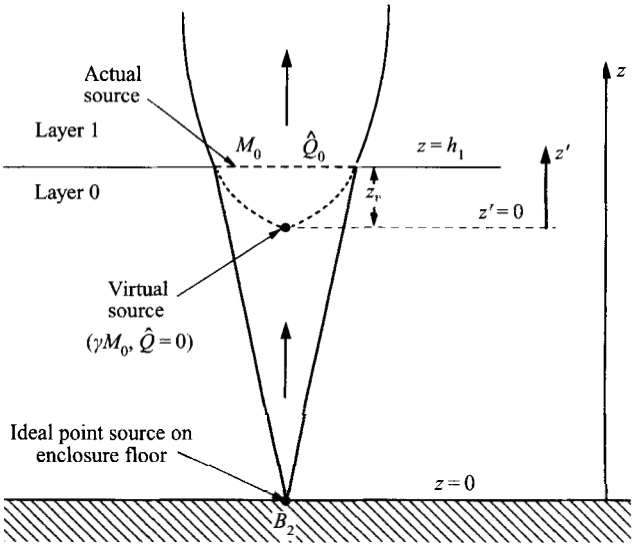

FIGURE 2. Definition sketch of stronger plume passing through layer 1.

where the quantities $\hat{Q} = Wb^2 (= Q/\pi)$, $M = (Wb)^2$ and $F = g'\hat{Q} (= B/\pi)$ are proportional to the volume flux, the specific momentum flux and the buoyancy flux, respectively, in the plume of radius b and vertical velocity W. Eliminating z from (19) gives

$$M^{3/2}\,\mathrm{d}M = \frac{F}{2\alpha}\hat{Q}\,\mathrm{d}\hat{Q}, \tag{20}$$

and hence

$$\tfrac{2}{5}(M^{5/2}(z) - M^{5/2}(0)) = \frac{F}{4\alpha}(\hat{Q}^2(z) - \hat{Q}^2(0)). \tag{21}$$

A source at $z = h_1$ of finite volume flux, $\hat{Q}_0$, and momentum flux, M_0, may be modelled as originating from a 'virtual source' of finite momentum flux, γM_0, but zero volume flux. This is situated at some distance z_v below the actual source and γ is a dimensionless quantity whose value is to be determined. Using a second coordinate $z' = z + z_v - h_1$, and rearranging (21) we then have

$$M(z') = \left(\frac{5F}{8\alpha}\hat{Q}^2(z') + (\gamma M_0)^{5/2}\right)^{2/5}. \tag{22}$$

Applying (22) at $z = h_1$ (i.e. $z' = z_v$) when $M(z') = M_0$ and $\hat{Q}(z') = \hat{Q}_0$ we obtain

$$\gamma = \left(1 - \frac{5F}{8\alpha}\frac{\hat{Q}_0^2}{M_0^{5/2}}\right)^{2/5}. \tag{23}$$

In the present situation plume 2 originates from an ideal point source at $z = 0$ of strength $B_2 (= \pi F_2)$ with zero volume flux and momentum flux, and (22) reduces to

$$M_0^{5/2} = \frac{5F_2}{8\alpha}(\hat{Q}_0(z))^2. \tag{24}$$

So for plume 2 at height $z > h_1$ from the floor the distributed source buoyancy flux in Layer 1 is B_2' where, from (24)

$$\frac{B_2'}{B_2} = \frac{F_2'}{F_2} = \frac{5F_2'}{8\alpha}\frac{\hat{Q}_0^2}{M_0^{5/2}}. \tag{25}$$

From (9), (11) and (13) we have

$$B_2'/B_2 = (1-\psi^{2/3}). \tag{26}$$

Substituting (25) into (23) we find

$$\gamma = (1-B_2'/B_2)^{2/5},$$

and so, from (26)

$$\gamma = \psi^{4/15}. \tag{27}$$

Thus, the plume passing through the interface at $z = h_1$ behaves as though it arises from a point source at $z = h_1 - z_v$, with buoyancy flux B_2' and momentum flux $\psi^{4/15}M_0$. To close the problem the volume flux Q_{22} across the top interface is required in terms of h_1, h_2, B_1 and B_2. Using (22) equation (19*a*) may be written as

$$\frac{\mathrm{d}\hat{Q}}{\mathrm{d}z'} = 2\alpha\left(\frac{5F_2'}{8\alpha}\hat{Q}^2(z') + (\gamma M_0)^{5/2}\right)^{1/5},$$

$$= (20\alpha^4 F_2')^{1/5}(\hat{Q}^2(z') + \hat{q}^2)^{1/5}, \tag{28}$$

where

$$\hat{q} = \hat{Q}_{21}\left(1-\left(\frac{B_2'}{B_2}\right)\right)^{1/2}\left(\frac{B_2'}{B_2}\right)^{-1/2}$$

$$= \frac{\hat{Q}_{21}\psi^{1/3}}{(1-\psi^{2/3})^{1/2}}. \tag{29}$$

The position of the virtual source is then given by

$$z_v = \frac{\hat{q}^{3/5}}{(20\alpha^4 F_2')^{1/5}}\int_0^{\hat{Q}_0/\hat{q}} \frac{\mathrm{d}t}{(t^2+1)^{1/5}}. \tag{30}$$

The volume flux in the strong plume entering layer 2 is determined from (28), and hence,

$$\frac{h_2}{h_1} = 1 - \frac{z_v}{h_1} + \frac{1}{(20\alpha^4 F_2)^{1/5}}\frac{1}{h_1}\int_0^{\hat{Q}_{22}} \frac{\mathrm{d}\hat{Q}}{(\hat{Q}^2+\hat{q}^2)^{1/5}}, \tag{31}$$

$$f(\psi) = \frac{3}{5}\frac{\psi^{1/5}}{(1-\psi^{2/3})^{1/2}}\int_a^b \frac{\mathrm{d}t}{(t^2+1)^{1/5}}, \tag{32}$$

where

$$b = \frac{(1+\psi^{1/3})(1-\psi^{2/3})^{1/2}}{\psi^{1/3}}, \quad a = \frac{(1-\psi^{2/3})^{1/2}}{\psi^{1/3}}.$$

The expression for f given by (32) is consistent with the postulated form (17) that $f = f(\psi)$ and provides a posteriori justification for the assumed form of the ratio of the layer thicknesses.

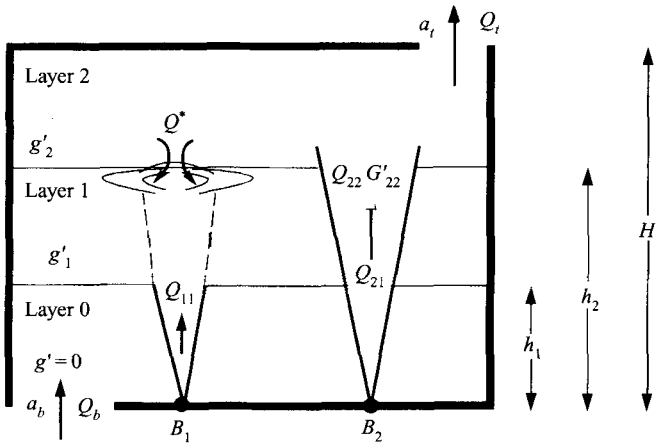

FIGURE 3. Theoretical model of entrainment of fluid from layer 2 by weaker plume (after Kumagai 1984).

The interface heights for a given situation are determined from (18) and (32). In addition, the layer densities may be found as follows. The density of layer 1 is dependent on the magnitude of the source strengths and is given by (9). However, the buoyancy of layer 2 relative to layer 1 is a function of the ratio of buoyancy fluxes only. Using equations (6), (7) and (15) the layer buoyancy ratio g'_1/g'_2 is given by

$$\frac{g'_1}{g'_2} = \frac{(\psi + \psi^{2/3})}{(1+\psi)}. \tag{33}$$

2.3. *Entrainment from the top layer by the weaker plume*

The theoretical model above gives good qualitative agreement with experimental results for relatively low values of ψ as it stands. However, it does not account for the fact that fluid is entrained from layer 2 into layer 1 by impingement of the weaker plume on the interface between these two layers, and we now consider how this entrainment may be incorporated into the analysis described above. The experiments, which we describe later, show that once fluid from the weaker plume has passed through the interface between layers 0 and 1, it continues in the form of a weak jet until it impinges on the upper interface. This situation is very similar to that investigated by Baines (1975) and Kumagai (1984). These authors quantified the volume and buoyancy fluxes resulting from entrainment by a plume impinging on a density interface. In the present case, the effect of the weak jet is to raise the level of the upper interface by entraining a given volume flux, Q^*, of the more buoyant fluid from the top layer. The situation is shown schematically in figure 3, and gives rise to a modification to the relations (5) and (6) for conservation of volume and buoyancy fluxes, respectively, such that

$$Q_t = Q_b = Q_{22} - Q^* = Q_{11} + Q_{21}, \tag{34}$$

$$B_1 + B_2 = Q_{11}\,G'_{11} + Q_{21}\,G'_{21} = (Q_{22} - Q^*)\,G'_{22}. \tag{35}$$

In practice, this entrainment flux will result in the generation of a density gradient in the upper part of layer 1 as reported by Kumagai. However, this will not affect the locations of the interface heights between the three layers, nor the mean densities in each layer and consequently we maintain the assumption that layer 1 is fully mixed for the purposes of the present analysis.

Both Kumagai and Baines found that the volume of fluid entrained when a plume impinges on a density interface is a function of a Froude number, Fr^*, based on the velocity, w, and radius, r, of the plume and on the difference in density between the two layers concerned, $\Delta g'$. In the present case we assume that this Froude number is determined by the velocity and radius of the weaker plume assuming it rises to the upper interface over height h_2 through ambient fluid only. This simplification removes the necessity to model the complexities of the weak jet development in layer 1 explicitly. Thus,

$$Fr^* = \frac{w_{12}}{(r_{12}(g_2' - g_1'))^{1/2}}. \tag{36}$$

This Froude number is then determined from relations already developed above and from the theory of Morton *et al.* (1956). The weaker plume velocity and radius assuming a point source and top hat profiles are then

$$w_{12} = \left(\frac{5}{6\alpha}\right)\left(\frac{9}{10}\alpha\right)\left(\frac{B_1}{\pi}\right)^{1/3} h_2^{-1/3}, \quad r_{12} = \left(\frac{6\alpha}{5}\right)h_2, \tag{37}$$

respectively. From (9), (33), (36) and (37) we then have

$$Fr^* = \left(\frac{5}{8\alpha}\right)^{1/2}\left(\frac{\xi_1}{\xi_2}\right)^{5/6}\left(\frac{\psi + \psi^{2/3}}{1-\psi^{2/3}}\right)^{1/2}. \tag{38}$$

We use the empirical correlation of Kumagai (1984) to determine the volume of fluid, Q^*, entrained at the upper interface. Thus,

$$Q^* = \Omega Q_{12} = \Omega(\xi_2/\xi_1)^{5/3} Q_{11}, \tag{39}$$

where

$$\Omega = \frac{Fr^{*3}}{1 + 3.1Fr^{*2} + 1.8Fr^{*3}}. \tag{40}$$

(Note that in Kumagai's original notation Q^* represented the volume flowrate divided by π.) The entrained fluid has the effect of raising the upper interface height and increasing Q_{22}. From (34) and (39) we have

$$Q_{22} = Q_{11}[(1 + \Omega(\xi_2/\xi_1)^{5/3}) + \psi^{-1/3}], \tag{41}$$

and $\Omega(\xi_2/\xi_1)^{5/3}$ is therefore a correction to be applied to the upper limit of (32) such that the limits of integration now become

$$b = \left[1 + \left(1 + \Omega\left(\frac{\xi_2}{\xi_1}\right)^{5/3}\right)\psi^{1/3}\right]\frac{(1-\psi^{2/3})^{1/2}}{\psi^{1/3}}, \quad a = \frac{(1-\psi^{2/3})^{1/2}}{\psi^{1/3}}. \tag{42}$$

2.4. *Results of the theoretical analysis*

Equations (18), (32) and (42) give the full solution to the problem. An important result is that the heights of the two interfaces, h_2 and h_1, are determined by only two parameters A^*/H^2 and the ratio of the source strengths, $\psi = B_1/B_2$. As in the case of a single plume, the heights of the interfaces are independent of the total strengths of the sources. This result reflects the fact that the interface positions are geometrical quantities and on dimensional grounds can only depend on these parameters. Furthermore, the ratio of the heights of the interfaces (h_2/h_1) is dependent only on ψ.

The magnitudes of the two non-dimensional interface heights, ξ_1 and ξ_2, are shown in figure 4 for two values of the geometric parameter A^*/H^2 with the constant C taken as 0.11. (Note that Turner (1986) suggests that a suitable value for the entrainment constant α determined by experiment assuming Gaussian profiles is $\alpha = 0.083$ giving $C = \frac{6}{5}\alpha(\frac{9}{5}\alpha)^{1/3}\pi^{2/3} = 0.11$). These results shown in figure 4 were obtained by simultaneous

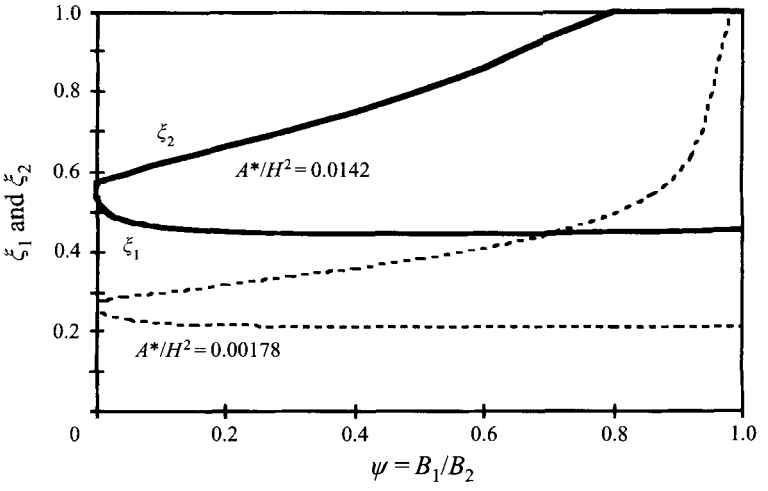

FIGURE 4. Theoretical prediction of the non-dimensional interface heights ξ_1 and ξ_2 as functions of the ratio B_1/B_2 of the buoyancy fluxes, for two different values of the dimensionless vent area A^*/H^2.

solution of (18), (32) and (42). When there is a single plume ($\psi = 0$), a single interface forms at the height predicted by (1). When the second plume is turned on, two interfaces are formed. The lower interface descends below the level of the original interface (when $\psi = 0$) while the upper interface is established above the original interface position. The descent of the lower layer occurs rapidly up to $\psi \approx 0.2$, after which there is little change in its elevation. When $\psi = 1$, this interface corresponds to the position predicted by (3) for $n = 2$. As ψ increases from zero the upper interface rises and the rate of change in h_2 with respect to ψ becomes increasingly steep as $\psi \to 1$. This is because entrainment of upper layer fluid by the weaker plume becomes increasingly important as both ψ and, consequently, Fr^* increase. For all non-dimensional vent areas, A^*/H^2, the upper interface eventually reaches the ceiling of the enclosure. At this point, the theoretical model predicts the absence of layer 2 and a two-layer stratification is re-established; i.e. fluid in plume 2 has sufficient buoyancy for the plume to reach the ceiling of the enclosure where it exits immediately. The height of the interface between layers 1 and 2 is then obtained by modifying the analysis above appropriately to account for the presence of only one buoyant layer.

The degree of stratification within the enclosure is an important consideration. The buoyancy of layer 1 may be predicted using equation (9) and is dependent on the magnitude of the buoyancy flux from source 1. Consider the situation where one plume, say B_2, is established and a two-layer steady stratification has built up. When a weaker plume $B_1 < B_2$ is turned on, a layer forms below the existing interface, as shown in figure 4. When $\psi = B_1/B_2$ is small the density step into this layer is small and the buoyancy of this layer increases with increasing B_1, since both the strength of the plume increases and the lower interface $z = h_1$ decreases in height. Consequently, the buoyancy of layer 1 increases relative to layer 2. As ψ increases further the elevation of the upper interface increases until it reaches the ceiling and only a single layer of buoyancy g_1' remains.

Figure 5 shows the variation in buoyancy of the two layers as functions of the flux ratio ψ. The ratio of the buoyancies of the two layers is independent of the strengths of the individual plumes for the three-layer stratification shown in figure 1, and this depends only on the ratio of the source buoyancy fluxes. The explicit form is given by

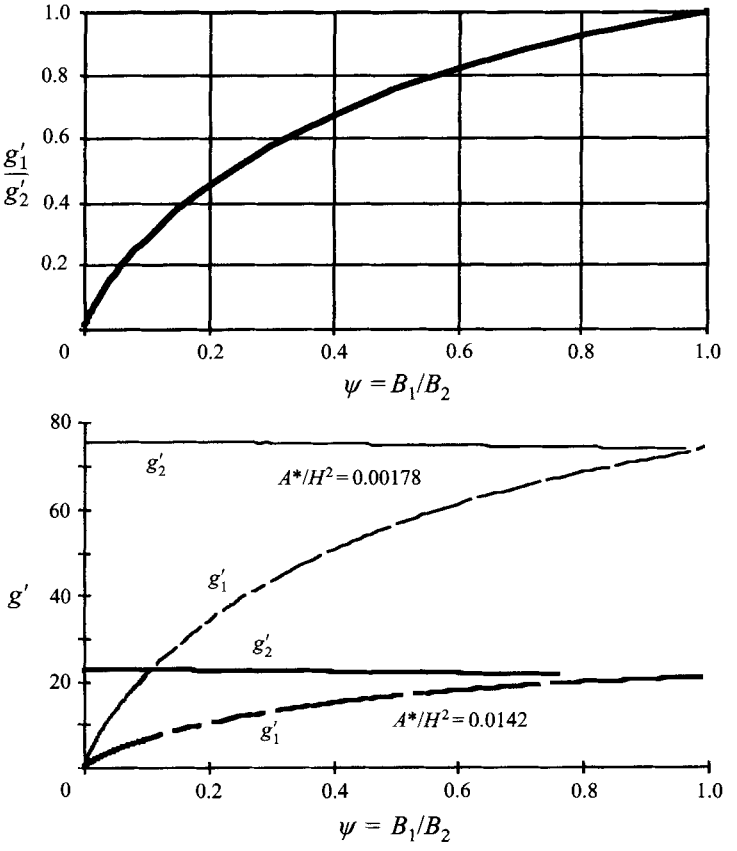

FIGURE 5. Theoretical prediction of layer buoyancies for two positive plumes. (*a*) Layer buoyancy ratio for any value of A^*/H^2, and total source strengths. (*b*) Layer buoyancies for fixed total buoyancy flux $(B_1 + B_2) = 1$ at two values of A^*/H^2. The units of g' are arbitrary.

(33) and this relationship is shown in figure 5(*a*). If, as a result of entrainment, the upper layer is mixed down by the weaker plume, as shown in figure 4 for $\psi \to 1$, then the upper-layer buoyancy is not defined for larger values of ψ. The buoyancy of each layer depends on the plume strength, and figure 5(*b*) shows the variation with the flux ratio ψ for two different values of A^*/H^2 when the total source strength $B_1 + B_2 = B$ is kept fixed. The results of the calculation obtained from (9), (18), (32), (33) and (41) for the full range of ψ in the two-plume case, show how the buoyancy of the two layers varies between these two extremes. As ψ increases, the buoyancy of layer 1 increases as the weaker plume flows into this layer, while that of the upper layer decreases as the buoyancy flux of the stronger plume decreases. The upper layer disappears at some upper limit of ψ, beyond which only g_1' is shown.

3. Two plumes with buoyancy of opposite sign

The second situation considered in this paper is where an enclosure contains two plumes, one of which is positively buoyant and the other is negatively buoyant, as shown schematically in figure 6. For the sake of definiteness we suppose that plume B_1 is of negative buoyancy, the second plume B_2 is of positive buoyancy, and that $B_1 < B_2$. As before, we denote the ratio of the buoyancy fluxes by $\psi \equiv B_1/B_2 \leqslant 1$. For Boussinesq plumes we can reverse the relative strengths of B_1 and B_2 by reversing

gravity. We take both B_1 and B_2 as positive and derive the conservation equations with due regard to the directionality of the plumes. It is postulated that three layers of fluid of different densities are formed as shown, and again this configuration has been confirmed by the experiments described in §4. Equation (4) is applicable to this situation and determines the flowrate through the enclosure given the stratification shown. In addition, there is entrainment of ambient fluid from layer 0 by the weaker plume as it impinges on the interface between layers 0 and 1 in a similar manner to the situation considered in §2.3. The following relations determine the behaviour of the system under steady-state conditions.

Conservation of volume flux requires that

$$Q_t = Q_b = Q_{21} + Q^* = Q_{22} - Q_{12}, \tag{43}$$

and conservation of buoyancy in the three layers is given by:

$$\text{Layer 0} \quad B_2 = G'_1 Q_{21} = \text{constant}, \tag{44}$$

$$\text{Layer 1} \quad B_2 + Q_{12} g'_1 = Q_{22} g'_2, \tag{45}$$

$$\text{Layer 2} \quad B_2 - B_1 = Q_t g'_2 = Q_{21} g'_2. \tag{46}$$

For the negatively buoyant (weaker) plume

$$B_1 = -G'_{12} Q_{12}, \tag{47}$$

$$Q_{12} = C(B_1 h_3^5)^{1/3}, \tag{48}$$

$$G'_{12} = g'_2 - \frac{1}{C}(B_1^2 h_3^{-5})^{1/3} = g'_1 = g'_2 - \frac{B_1}{Q_{12}}, \tag{49}$$

where the thickness of layer 2 is denoted by $h_3 = (H - h_2)$.

For the positively buoyant (stronger) plume in layer 0

$$B_2 = G'_{21} Q_{21} = \text{constant}, \tag{50}$$

$$Q_{21} = C(B_2 h_1^5)^{1/3}, \tag{51}$$

$$G'_{21} = \frac{1}{C}(B_2^2 h_1^{-5})^{1/3}. \tag{52}$$

Using an approach similar to that for two buoyancy sources of the same sign, the stronger plume has a reduced buoyancy flux, B'_2, relative to layer 1, given by (13). Thus,

$$B'_2/B_2 = \psi + \psi^{2/3}(h_1/h_3)^{5/3}, \tag{53}$$

which is equivalent to (26). (It is interesting to note that (53) implies a restriction on the range of h_1/h_3 for a given value of ψ since from physical considerations it is necessary that $B'_2/B_2 < 1$. If this restriction is not met then the flow regime illustrated in figure 6 no longer applies and this case is discussed further below.) The behaviour of the stronger plume in layer 1 is identical to that for the previous case and the ratio of interface heights is given by (17).

The volume of fluid entrained at the density interface between layers 0 and 1 is determined from the Froude number, Fr^*, based on the radius and velocity that the weaker plume would achieve were it to develop from the enclosure ceiling to h_1 through fluid of buoyancy g'_2. Thus,

$$Fr^* = \frac{w_{11}}{(r_{11} g'_1)^{1/2}} = \left(\frac{5}{8\alpha}\right)^{1/2} \left(\frac{1-\xi_2}{1-\xi_1}\right)^{5/6} \left[\left(\frac{h_3}{h_1}\right)^{5/3} (\psi^{-2/3} - \psi^{2/3}) - 1\right]^{-1/2}. \tag{54}$$

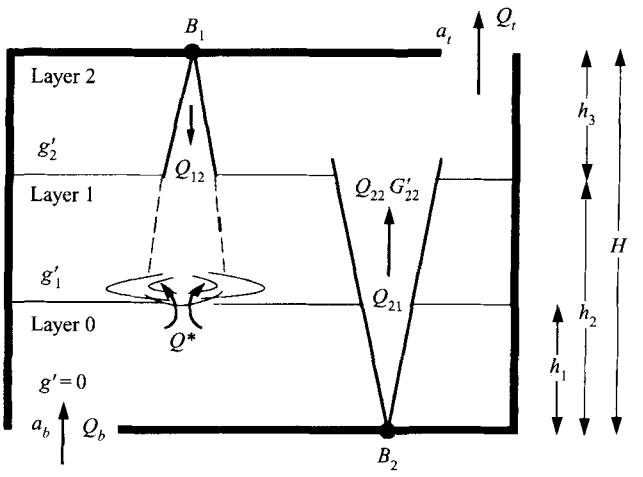

FIGURE 6. Ventilated enclosure with buoyancy sources of opposite sign.

In this case

$$Q^* = \Omega Q_{11} = \Omega\left(\frac{H-h_1}{H-h_2}\right)^{5/3} Q_{12}, \tag{55}$$

Equations (43), (48), (51) and (55) may be rearranged to obtain

$$Q_{22} = Q_{21}\left(1+\left[1+\Omega\left(\frac{1-\xi_1}{1-\xi_2}\right)^{5/3}\right]\psi^{1/3}\left(\frac{h_3}{h_1}\right)^{5/3}\right), \tag{56}$$

where Ω is given by (40) as before. In the present case (28) is again applicable and by using (53) and (56) the ratio of interface heights is then given by the function

$$f(\psi) = \frac{3}{5}\left(\frac{B_2}{B_2'}\right)^{1/5}\left(\frac{B_2}{B_2'}-1\right)^{3/10}\int_a^b \frac{\mathrm{d}t}{[t^2+1]^{1/5}}, \tag{57}$$

where

$$b = \left(1+\left[1+\Omega\left(\frac{1-\xi_1}{1-\xi_2}\right)^{5/3}\right]\psi^{1/3}\left(\frac{h_3}{h_1}\right)^{5/3}\right)\left[\left(\frac{B_2}{B_2'}\right)-1\right]^{-1/2}, \quad a = \left[\left(\frac{B_2}{B_2'}\right)-1\right]^{-1/2}.$$

The pressure balance equation equivalent to (18) is

$$\frac{A^*}{H^2C^{3/2}} = \left(\frac{\xi_1^5}{(1-\psi)(1-\xi_1)-\psi^{2/3}\left(\dfrac{\xi_1}{1-\xi_1(1+f(\psi))}\right)^{5/3} f(\psi)\,\xi_1}\right)^{1/2}. \tag{58}$$

The problem is then solved by simultaneous numerical solution of (57) and (58).

Again we find that the height of the two interfaces is determined solely by the geometry of the enclosure and the ratio of the strengths of the buoyancy sources, $\psi = B_1/B_2$. Results for one example of the situation shown in figure 6 are now discussed for a typical case with the non-dimensional area opening, A^*/H^2, taken to be 0.001. Consider first the situation with a single source, B_2, operating, i.e. $\psi = 0$, when only one interface is present at $\xi = 0.22$. If a weak negative source is then introduced at the top of the enclosure the resulting plume passes through almost all the original buoyant layer to form a thin layer (layer 1) at $\xi_1 \approx 0.22$. The depth of this layer increases rapidly with increasing ψ, i.e. ξ_2 increases rapidly while ξ_1 decreases steadily as shown quantitatively in figure 7.

The flow regime in the enclosure in the case of two plumes of opposite sign has three possible configurations. The three layers shown in figure 6 only exist in this

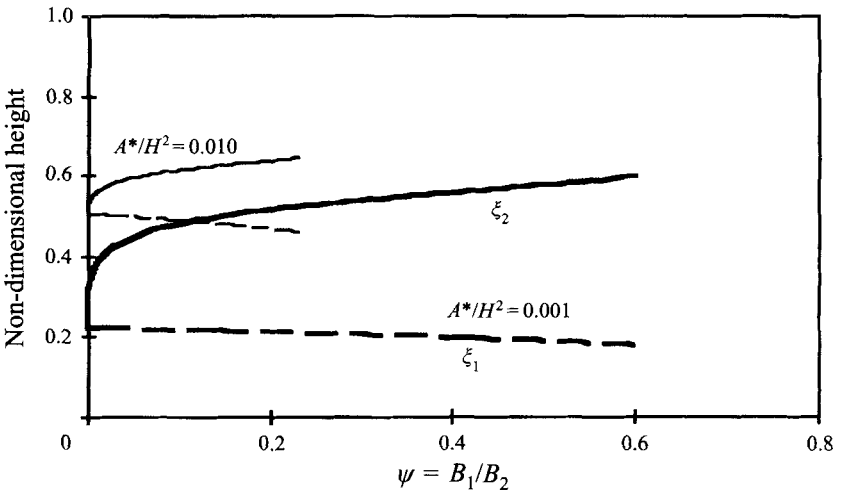

FIGURE 7. Theoretical prediction of interface heights for sources of opposite sign at two values of A^*/H^2 for the flow regime of figure 6.

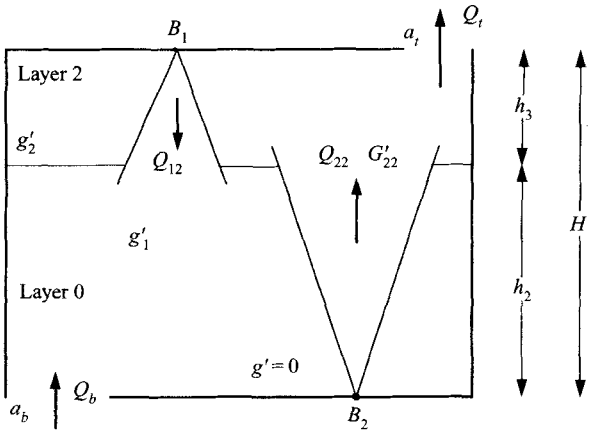

FIGURE 8. Ventilated enclosure with buoyancy sources of opposite sign at the limiting condition $B_2'/B_2 = 1$.

configuration up to a value of ψ corresponding to $B_2'/B_2 = 1$. At this limiting condition a second flow configuration applies where the weaker source has sufficient buoyancy flux to supply layer 1 with fluid of density equal to that of the ambient fluid as shown schematically in figure 8. In this case the lower interface at $z = h_1$ disappears. At this limiting condition the ratio of plume source strengths is given by

$$h_1/h_3 = (\psi^{-2/3} - \psi^{1/3})^{3/5}. \tag{59}$$

Two sets of results for ξ_1 and ξ_2 are shown in figure 7. Higher values of A^*/H^2 lead to a more limited range of ψ in which the flow configuration of figure 6 is possible. For values of ψ greater than the critical condition, the negatively buoyant plume is sufficiently strong to form a layer of fluid denser than ambient at the bottom of the enclosure corresponding to a third flow configuration which is illustrated in figure 9. In this case there is a two-way flow through the bottom vent, a_b, and ambient fluid from

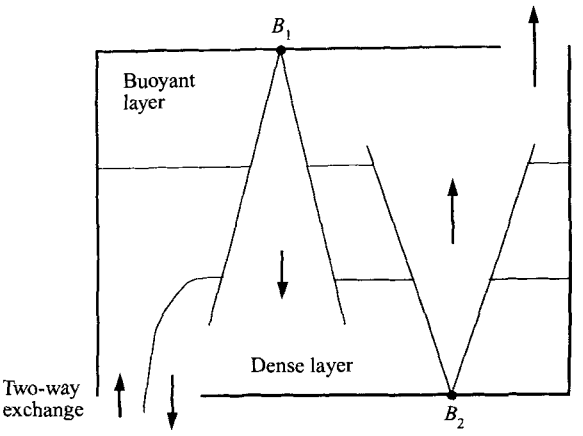

FIGURE 9. Ventilated enclosure with buoyancy sources of opposite sign for high values of B_1/B_2.

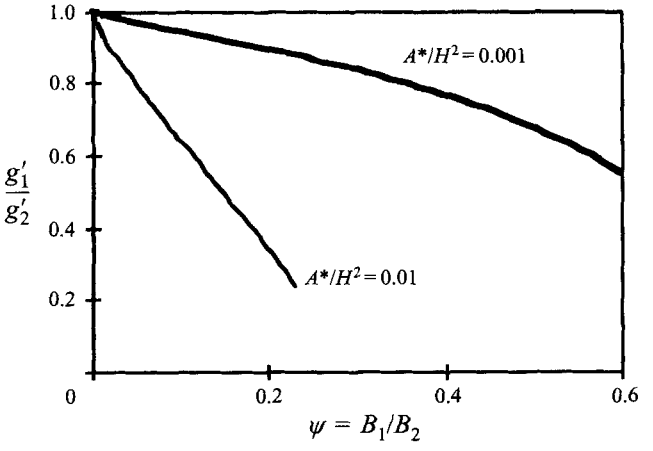

FIGURE 10. Theoretical prediction of stratification, g_1'/g_2', in an enclosure with sources of opposing buoyancy, for $A^*/H^2 = 0.001$ and 0.01.

this source rises as a plume to supply fluid for the middle layer of density slightly greater than ambient. Owing to the complex nature of the exchange flow through the lower opening this case is not discussed further here.

For the three-layer flow shown in figure 6 the density of the two upper layers in the enclosure may be found from the magnitude of the buoyancy flux and volume flux of the plume entering the layer of the same density. A convenient measure of the stratification in the enclosure is the ratio g_1'/g_2' which may be found from (46) and (48–50) as

$$\frac{g_1'}{g_2'} = 1 - \frac{\psi^{2/3}}{(1-\psi)}\left(\frac{\xi_1}{1-\xi_2}\right)^{5/3}. \tag{60}$$

As in the case with sources of buoyancy of the same sign, the ratio of layer densities is dependent only on the relative strength of the sources. Figure 10 shows the stratification in the enclosure corresponding to the interface heights shown in figure 7, for the particular cases of $A^*/H^2 = 0.001$ and 0.01.

4. Experimental results

The mathematical models derived above have been tested against experiments using a naturally ventilated Perspex enclosure, 250 mm high, 450 mm long and 350 mm wide, with water as the working fluid. The enclosure was suspended in a large tank of water to ensure there was no change in density of the ambient fluid throughout the course of an experiment. Negative sources of buoyancy were generated using concentrated sodium chloride solution injected through nozzles in the floor of the enclosure, and a number of openings were available in the floor and ceiling of the enclosure to allow a wide range of values of A^*/H^2 to be obtained. The salt solution was supplied to the sources from a constant head, gravity fed system. Flow rates were controlled by means of needle valves and measured with rotameters which were calibrated at the start of each experiment. Considerable care was taken in the design of the source nozzles to ensure that the plumes were both turbulent and of low Froude number. Upstream of the 5 mm diameter outlet, each source comprised a narrow restriction in the flow followed by a fine wire mesh. The fluid flow and interface heights within the enclosure were visualized using a shadowgraph technique. Further details of the experimental techniques employed may be found in Linden *et al.* (1990).

All experimental data presented below were measured under steady-state conditions. Equilibrium was generally achieved after approximately fifteen minutes following a change in any of the experimental parameters.

4.1. *Two-plumes with buoyancy of the same sign*

The flow regime illustrated in figure 1 was found to occur in all experiments with two positive sources of buoyancy. Figure 11 shows shadowgraph images of the steady flow for the case of a single plume (figure 11*a*) and two unequal plumes (figure 11*b*). The experimental enclosure has openings in the top and bottom, and the accumulation of buoyant fluid at the top of the enclosure produces pressure differences which cause inflow of ambient fluid through the lower openings and outflow through the upper openings. Upwards displacement ventilation occurs in both cases, but the form of the internal stratification is different in the two cases. (The photographs have been inverted to illustrate the effects of positive sources of buoyancy, although in practice these plumes are produced by dense salt solution.)

For the case of a single plume (figure 11*a*) the stratification consists of two uniform layers separated by a single stable density interface. This interface is observed to be quite sharp, and fluid only crosses it from the lower to the upper layer in the plume. This situation has been discussed in detail in Linden *et al.* (1990). When a second (weaker) plume is added, fluid from this plume rises through the ambient lower layer and crosses the interface. However, once in the upper layer this plume is no longer positively buoyant, and this fluid spreads out along the interface forming an intermediate layer. This situation is shown in figure 11(*b*). The stronger plume now passes through the two interfaces and discharges into the upper layer. Comparison of figures 11(*a*) and 11(*b*) shows that, as a result of the second plume, the lower interface $z = h_1$ reduces in height while the new interface forms above the position of the original interface. These results are consistent with the theoretical predictions shown in figure 4.

If the second plume had been stronger than the original plume the time development of the stratification would have been different. In that case the fluid from the new plume rises to the top of the enclosure producing a new interface. The fluid from the original plume now no longer reaches the top of the enclosure but stops below the new

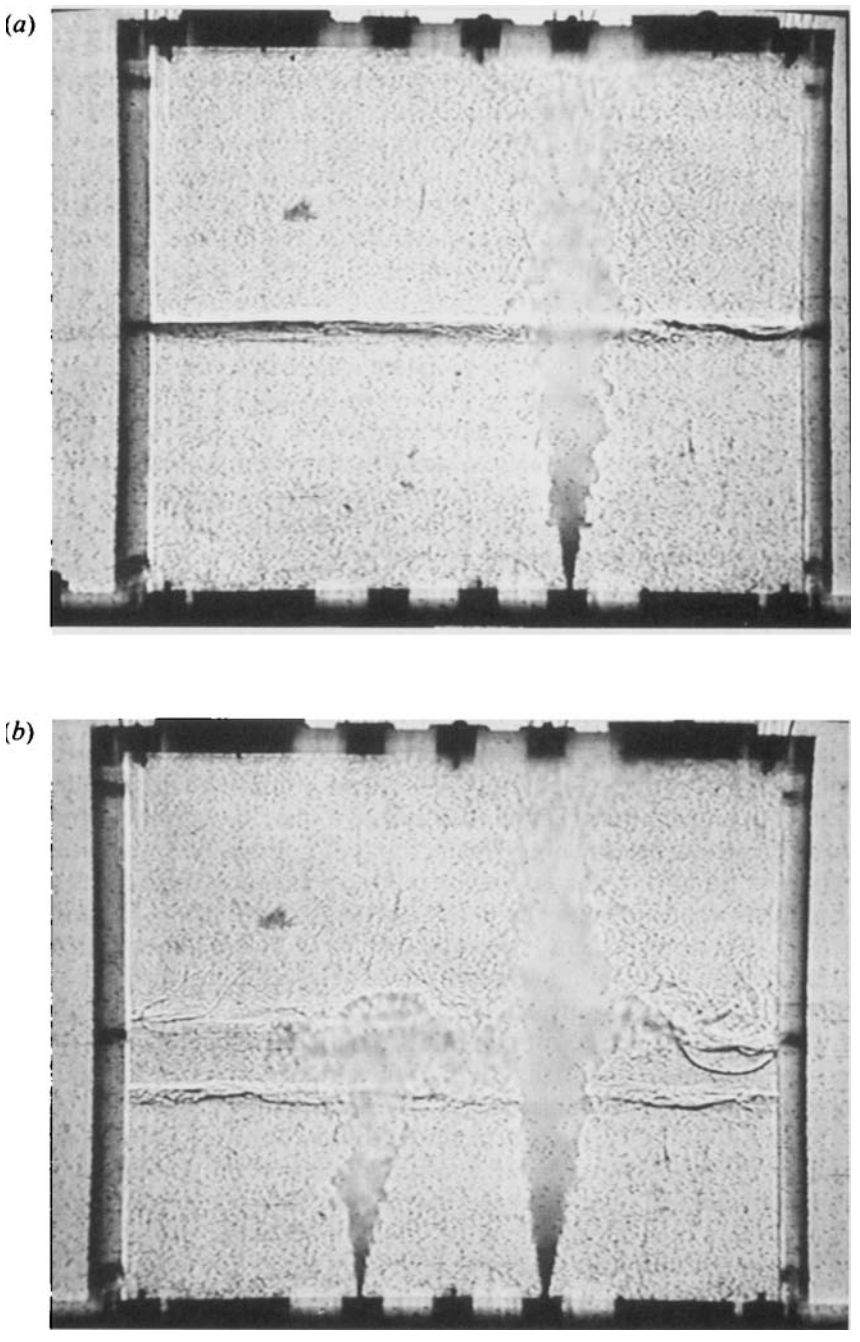

FIGURE 11. Shadowgraphs of flow within the enclosure containing (*a*) a single source of buoyancy and (*b*) two sources of buoyancy of the same sign.

interface. Entrainment by the stronger plume drains fluid from the intermediate layer (layer 1) until the equilibrium interface positions are attained. If both plumes are turned on at the same time in an enclosure containing initially uniform fluid, both plumes initially reach the top of the enclosure. As the buoyant fluid develops at the top of the enclosure the weaker plume stops at an intermediate depth, and the three-layer

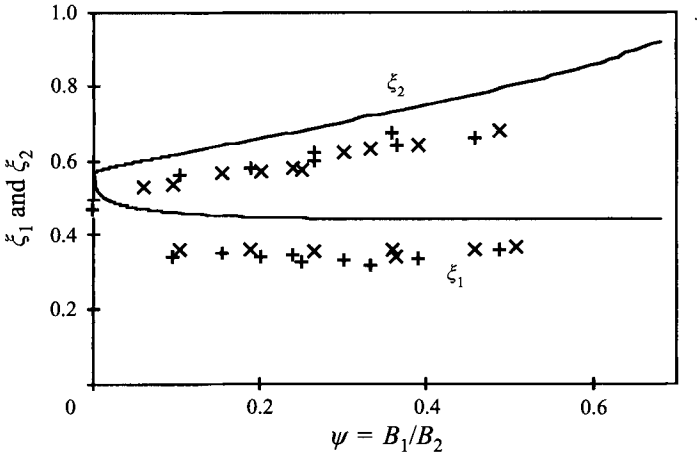

FIGURE 12. Non-dimensional interface heights ξ_1 and ξ_2 for the lower and upper interface, respectively, plotted against B_1/B_2, the ratio of the buoyancy fluxes, for two negative sources of buoyancy. ($A^*/H^2 = 0.0142$. Experimental results for sources with finite volume fluxes: × Source 2, volume flux = 2.66 ml s^{-1}, $g' = 71$ cm s^{-2}; + Source 2, volume flux = 2.47 ml s^{-1}, $g' = 147$ cm s^{-2}. Solid lines, theoretical results.)

stratification is again established. The final interface positions are observed to be the same irrespective of the transient behaviour. The interface between layers 0 and 1 was generally very stable and sharp. The second interface at $z = h_2$ was less distinct and exhibited variability in position owing to turbulence induced by the plumes.

Figure 12 shows experimental results of the interface heights for two plumes of negative buoyancy. The cross-sectional area of the ventilation openings in the enclosure was such that $A^*/H^2 = 0.0142$, and the data shown include two sets of experiments with nozzle diameters of 5 mm with buoyancy flux B_2 set to 1.90×10^{-6} (denoted by ×) and 3.63×10^{-6} m^4 s^{-3} (denoted by +), respectively. The maximum salt solution volume flow rate to each source was 2.66 cm^3 s^{-1} and the Froude number for each plume source did not exceed 6.0 (i.e. the plumes were very close to 'pure' or unforced plumes). The areas of the enclosure vents were chosen such that $a_t \ll a_b$ to minimize the effects of the small volume flux through the sources on flow through the vents. The results of figure 12 show how height of the lower interface ξ_1 decreases, while the height ξ_2 of the upper interface rises, as the relative strength of the weaker plume increases. The collapse of the data despite the two-fold variation in the buoyancy flux strongly supports the theoretical result that the interface heights depend only on the ratio of the buoyancy fluxes, $\psi = B_1/B_2$, and not on the total strength of the plumes.

Also shown in figure 12 are the theoretical curves for the non-dimensional interface heights ξ_1 and ξ_2, respectively, for this value of opening area plotted against the ratio of buoyancy fluxes ψ. There is good qualitative agreement with the theoretical analysis of §2. However, there is a slight offset between theoretical and experimental interface height results. The reason for this discrepancy is that in the experiments the buoyancy sources used were not 'ideal point sources' as they possessed both finite volume flux and momentum flux M at the source, despite having low Froude number. Hence, the quantitative interface heights differed to some extent from those predicted using the mathematical models described above. The most important effect of the departure of the non-ideal sources in the present case from point sources is the additional volume flux in the plumes at a given height. From forced plume theory, the virtual sources where the volume flux is zero of the experimental plumes are located 10–30 mm below

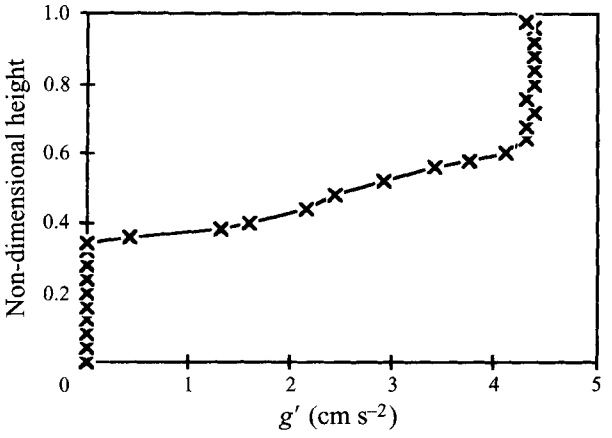

FIGURE 13. Stratification within the enclosure for two negative sources of buoyancy, $A^*/H^2 = 0.0142$ and $\psi = 0.25$.

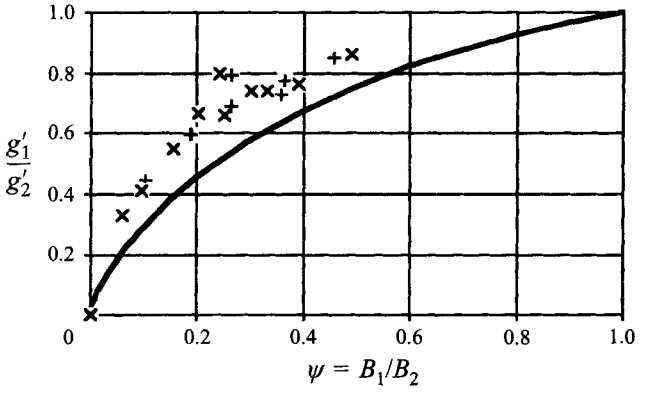

FIGURE 14. Comparison of experimental and theoretical layer buoyancy ratios for $A^*/H^2 = 0.0142$. Experimental results for sources with finite volume fluxes: ×, source 2, volume flux = 2.66 cm³ s⁻¹, $g' = 71$ cm s⁻²; +, source 2, volume flux = 2.47 cm³ s⁻¹, $g' = 147$ cm s⁻². Solid line, theoretical results.

the actual sources. This results in an offset between the theory and experiments of the order $\Delta\xi \sim 0.05-0.12$. When this is taken into account the experimental results match the theory very closely.

In §2.3 it was postulated that the entrainment of the upper buoyant layer by the weaker plume would lead to a degree of stratification within layer 1 as the buoyant fluid from the top layer is mixed down into the upper part of layer 1. The presence of this stratification has been confirmed experimentally. Figure 13 shows a plot of the buoyancy as determined by a conductivity probe calibrated against solutions of known salt concentration and traversed over the entire height of the enclosure. It is clear that the upper layer is well mixed while the less buoyant layer has a somewhat non-uniform stratification with a sharp density step at the interface with the ambient fluid. In view of this elimination of a sharp interface between the two buoyant layers at higher values of ψ experimental results for h_2 have only been reported in figure 12 where it was possible to clearly identify this interface visually (i.e. for $\psi < 0.5$).

The buoyancy ratio, g_1'/g_2', for the two layers was determined experimentally as a function of ψ and compared to that given by (33). These results are shown in figure 14

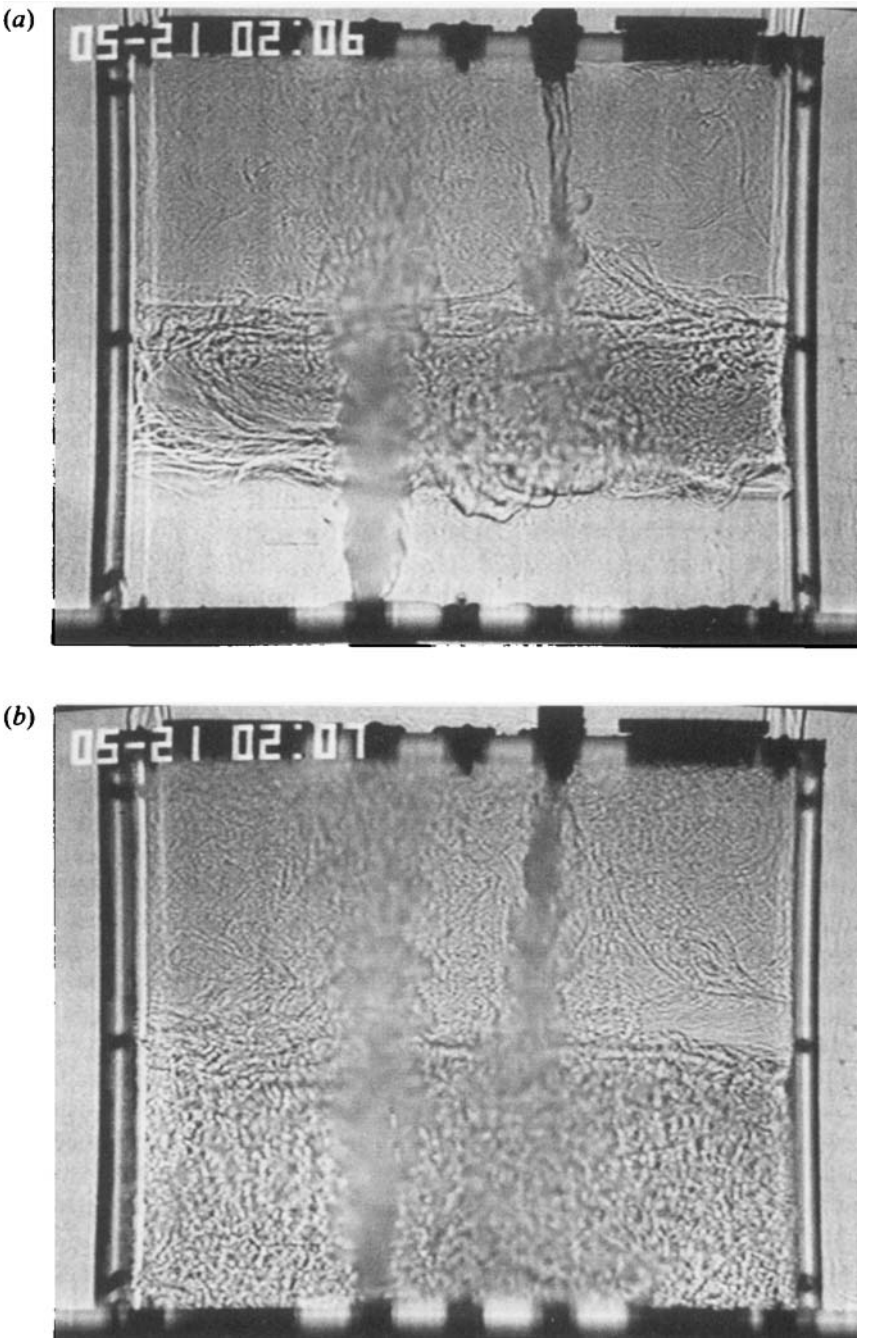

FIGURE 15. Shadowgraphs of flow within the enclosure generated by two sources of buoyancy of the opposite sign. (*a*) Three-layer stratification observed when $B_2'/B_2 < 1$. (*b*) Two-layer stratification observed when the two plumes have equal strength.

where the buoyancy of each layer was measured using a conductivity probe positioned at approximately the middle of each layer. The experimental results for the two buoyancy fluxes collapse onto a single curve and show quite good qualitative agreement with the theoretical analysis.

4.2. *Two plumes with buoyancy of opposite sign*

Experiments were also carried out with buoyancy sources of opposite sign. Positive buoyancy sources were produced by injecting a mixture of water and methylated spirit into the enclosure. Figure 15 shows an example of the flow. Figure 15(*a*) shows the three-layer stratification that develops when the second plume is sufficiently weak. (Note that in this case the photographs have also been inverted, so that the stronger plume is positively buoyant.) In this case, if the strong plume is established first a two-layer stratification with the associated displacement ventilation flow develops. When the weaker, negatively buoyant plume is turned on fluid descends and penetrates across the interface. In the lower layer this fluid is buoyant because it has entrained buoyant fluid from the upper layer as it decends, and it spreads out below the interface. Thus a new interface is established below the original interface. Fluid is carried downward across the upper interface by the negatively buoyant plume, and the thickness of the top layer decreases causing the upper interface to rise. This behaviour is consistent with the theoretical predictions shown in figure 7.

If the weaker negatively buoyant plume is established first, a two-layer stratification is again produced, but this time the displacement ventilation flow is in the opposite sense – with flow of dense fluid out of the bottom and ambient fluid in at the top. When the stronger positively buoyant plume is turned on, buoyant fluid accumulates at the top of the enclosure and the negative buoyancy of the fluid in the enclosure decreases. Eventually the average buoyancy within the enclosure becomes positive and the ventilation flow reverses. Ambient fluid then enters through the lower openings and, as this fluid is less dense than the fluid at the bottom of the enclosure, it produces a number of buoyant plumes which mix with the fluid in the enclosure in a complicated manner. Finally an upward displacement ventilation flow is established and the final steady state is as before.

Since the interface height for a single plume depends on the relative sizes of the upper and lower openings (Linden *et al.* 1990), it is not a simple matter to discuss the evolution when the sign of the ventilation flow changes. A further complication is shown in figure 15(*b*), which illustrates the flow when the two plumes have equal strengths. In this case the average buoyancy within the enclosure is zero and there is no net exchange with the exterior.

All three flow configurations described in §3 were observed, but, since the exchange flow through the lower opening is a complex flow in itself, only the situation shown in figure 6 was studied in detail. Experimental data are presented in figure 16 for two different non-dimensional enclosure opening areas. In contrast to the experiments discussed in §4.1, these experiments involved plumes that were significantly forced. The nozzle diameters for positive and negative sources were 2.2 mm and 1.8 mm, respectively, the range of buoyancy fluxes was between 3×10^{-7} and 2×10^{-6} m^4 s^{-3}, and the source Froude numbers did not exceed 60. The positive (salt solution) source was the stronger of the two sources in all experiments. The steady increase in h_2 and decrease in h_1 with increasing ψ is apparent. The second (critical) flow configuration was observed in each case, though the precise value of ψ at which this occurred was difficult to determine. This was in part due to the fact that as ψ increased the net buoyancy flux into the enclosure was reduced and the volume flux through the top and bottom vents became very small, and the time required to reach steady-state conditions was considerable. Again these dimensionless interface heights collapse onto a single curve for each value of A^*/H^2, showing that the interface heights are independent of the strengths of the sources. The offset in interface height found analytically and

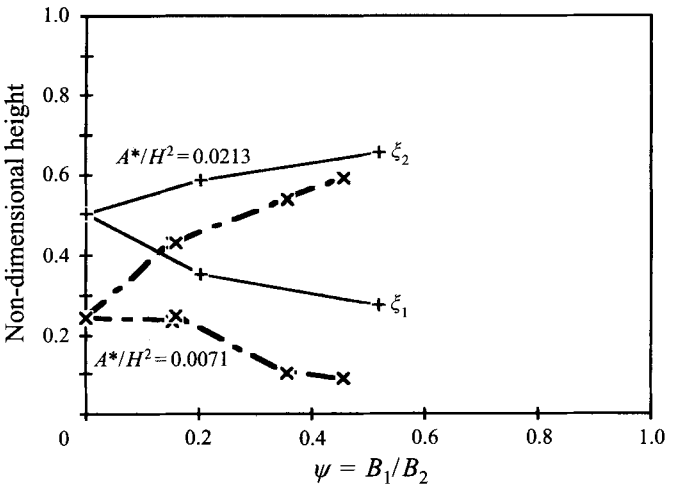

FIGURE 16. Non-dimensional interface heights ξ_1 and ξ_2 for the lower and upper interface, respectively, plotted against ψ for two sources of opposite sign. (Buoyancy fluxes range between 3×10^{-7} and 3×10^{-6} m^4 s^{-3}.)

experimentally (comparing figures 7 and 16) is again due to the real buoyancy sources possessing significant volume and momentum fluxes.

5. Conclusions

The behaviour of naturally ventilated enclosures containing two buoyancy sources has been investigated through analysis and experiment. A model to predict the thermal stratification within such enclosures has been developed based on the theory of flow in 'forced' plumes and also incorporates the effects of entrainment by a plume impinging on a density interface. It has been found that when two buoyancy sources of the same sign are present within an enclosure stratification develops in the form of three layers of different densities. The position of the interfaces between these layers is determined by the geometrical parameter A^*/H^2 and the *ratio* of strengths of the sources of buoyancy B_1/B_2 but not the absolute strength of the sources. The density of each layer is a function of the absolute strengths of the sources and the physical scale of the system.

An enclosure with two buoyancy sources of opposite sign shows similar but rather more complex flow characteristics. For low values of the parameter B_1/B_2 three layers are formed. However, there is a limiting condition for this configuration; i.e. at a given value of B_1/B_2 the two layers of density differing from that of the ambient fluid merge to form a single layer. Higher values of B_1/B_2 produce a more complex flow pattern with two of the three layers having density less than the ambient fluid.

The main conclusion of this paper is that two unequal plumes produce a three-layer stratification, and that the heights of the interfaces are solely determined by the dimensionless area of the openings and the ratio of the plume buoyancy fluxes. The simplifying result that the height of the stratified zone is independent of the total buoyancy flux into an enclosure with displacement ventilation produced by a single source of buoyancy is shown here to extend to the case of two unequal plumes. This generalization is predicted by the theoretical model (as well as on dimensional grounds), and is well supported by the laboratory experiments. It seems likely that this result will hold for any number of buoyant sources.

The theoretical models described in §2 may be used to predict stratification profiles in naturally ventilated enclosures providing the sources of buoyancy can be modelled as point sources on the floor of the building. Alternatively, where sources of finite volume and momentum flux are concerned, forced plume theory may be used to predict the stratification in the enclosure. Several limitations as to the application of the theoretical models must be borne in mind. These concern the inherent assumptions that: (*a*) plumes do not interact as they rise; (*b*) the aspect ratio of the enclosure is not extreme.

The analysis in this paper shows that it is possible to calculate exactly the flow due to two unequal plumes within a naturally ventilated enclosure. The steady-state configuration consists of three layers of different densities and, in the case of upward displacement ventilation, the lower layer is at ambient density. From the practical point of view it is important to estimate the height of this lowest interface and we see from figure 4 that its position depends only weakly on the ratio of the buoyancy fluxes B_1/B_2 and, over much of the range, is well predicted by the case of two plumes of equal buoyancy given by (3). The positions of the interfaces are determined primarily by the entrainment into the plumes and, consequently, are controlled by the volume fluxes in each plume. The plume volume flux is a strong function of the distance from the source but only a weak function of the buoyancy flux (see (8)). This is the reason why the lower interface position is relatively insensitive to the buoyancy flux ratio, and it seems possible to obtain a reasonable estimate of this interface height without evaluating the buoyancy flux exactly. This is the approximation that we employ in Linden & Cooper (1996) to calculate the stratification for multiple plumes within an enclosure.

REFERENCES

Baines, W. D. 1975 Entrainment by a plume or jet at a density interface. *J. Fluid Mech.* **68**, 309–320.

Caulfield, C. P. 1991 Stratification and buoyancy in geophysical flows. PhD thesis, University of Cambridge, UK.

Cooper, P. & Mak, N. 1991 Thermal stratification and ventilation in atria. *Proc. ANZSES (Australian and New Zealand Solar Energy Soc.) Conf., Adelaide, Australia*, pp. 385–391.

Gorton, R. L. & Sassi, M. M. 1982 Determination of temperature profiles in a thermally stratified, air-conditioned system: Part 2. Program description and comparison of computed and measured results. *Trans. ASHRAE*, **88** (2), paper 2701.

Jacobsen, J. 1988 Thermal climate and air exchange rate in a glass covered atrium without mechanical ventilation related to simulations. *13th Natl Solar Conf. MIT, Cambridge, MA*, vol. 4, pp. 61–71.

Kumagai, M. 1984 Turbulent buoyant convection from a source in a confined two-layered region. *J. Fluid Mech.* **147**, 105–131.

Linden, P. F. & Cooper, P. 1996 Multiple sources of buoyancy in a naturally ventilated enclosure. *J. Fluid Mech.* **311**, 177–192.

Linden, P. F., Lane-Serff, G. F. & Smeed, D. A. 1990 Emptying filling boxes: the fluid mechanics of natural ventilation. *J. Fluid Mech.* **212**, 309–335.

List, E. J. 1982 Turbulent jets and plumes. *Ann. Rev. Fluid Mech* **14**, 189–212.

Morton, B., Taylor, G. I. & Turner, J. S. 1956 Turbulent gravitational convection from maintained and instantaneous sources. *Proc. R. Soc. Lond.* A **234**, 1–22.

Morton, B. R. 1959 Forced plumes. *J. Fluid Mech.* **5**, 155–163.

Thomas, P. H., Hinkley, P. L., Theobald, C. R. & Simms, D. L. 1963 Investigations into the flow of hot gases in root venting. *Fire Res. Tech. Paper* 7, HMSO.

Turner, J. S. 1986 Turbulent entrainment: the development of the entrainment assumption, and its application to geophysical flows. *J. Fluid Mech.* **173**, 431–471.